Quantifying domain uncertainty in linear elasticity

Helmut Harbrecht, Viacheslav Karnaev, Marc Schmidlin

Departement Mathematik und Informatik
Fachbereich Mathematik
Universität Basel
CH-4051 Basel

Preprint No. 2023-06
June 2023

dmi.unibas.ch

Quantifying domain uncertainty in linear elasticity*

Helmut Harbrecht†, Viacheslav Karnaev†, and Marc Schmidlin†

Abstract. The present article considers the quantification of uncertainty for the equations of linear elasticity on random domains. To this end, we model the random domains as the images of some given fixed, nominal domain under random domain mappings, which are defined by a Karhunen-Loève expansion. We then prove the analytic regularity of the random solution with respect to the countable random input parameters which enter the problem through the Karhunen-Loève expansion of the random domain mappings. In particular, we provide appropriate bounds on arbitrary derivatives of the random solution with respect to those input parameters, which enable the use of state-of-the-art quadrature methods to compute deterministic statistics such as the mean and variance of quantities of interest such as the random solution itself or the random von Mises stress as integrals over the countable random input parameters in a dimensionally robust way. Numerical examples qualify and quantify the theoretical findings.

Key words. Uncertainty quantification, linear elasticity, regularity

MSC codes. 35R60, 60H35, 65C30

1. Introduction.

The equations which describe the behavior of elastic materials are widely studied in mechanics. Especially, the theory of linear elasticity is of interest and reasonable for many engineering materials and engineering design scenarios. The equations of linear elasticity considered in this article model the simplified behavior of an elastic material subject to surface and volume loads. The material is considered to be heterogeneous, especially allowing jumping material coefficients.

The numerical solution of the equations of linear elasticity are well understood if the input parameters are known. This, however, is often not the case in practical applications. If a statistical description of the input parameter is available, then one can mathematically describe data and solutions as random fields and aim at the computation of corresponding deterministic statistics of the unknown random solution. In this article, we consider uncertainties in the description of the computational domain. Applications are, besides traditional engineering, for example uncertain domains that derive from inverse methods such as tomography.

One possibility to account for the uncertainty in the domain is the linearization of the problem around a fixed, nominal domain with the help of techniques from shape calculus. Nonetheless, this *perturbation approach* introduces an error caused by the linearization. In particular, only small domain variations can be handled since the Eulerian setup is used. We refer the reader to [7, 13, 17] for example.

Therefore, we will consider another approach here, commonly refered to as the *domain mapping method*. For scalar, second order elliptic diffusion problems, this approach has been introduced in [26] and analysed in [4, 15]. Herein, it has been shown that the random boundary value problem's solution depends analytically on the random variation field under consider-

*Submitted to the editors June 11, 2023.

†Departement Mathematik und Informatik, Universität Basel, Spiegelgasse 1, 4051 Basel, Schweiz (helmut.harbrecht@unibas.ch, viacheslav.karnaev@unibas.ch, marc.schmidlin@unibas.ch).

ation. Respective Bayesian shape inversion has been studied in [9]. Higher-order regularity, required for multilevel quadrature methods, has been verified in [16]. Extensions to forward and inverse wave scattering problems are found in e.g. [8, 19, 20]. Finally, the domain mapping method has been applied for the stationary Navier-Stokes equation in [6].

Specifically, we consider the displacement field of an elastic body with a random boundary and with random inclusions. We choose to assume that part of its boundary is fixed while the rest is under external surface forces and, possibly, that the body is also subject to body forces. The material law we consider is that of linear elasticity, i.e., we assume that the forces yield small deformations or strains and that there is a linear relationship between the components of stress and strain. On the other hand, we model the random domains as the image of a given reference domain under a random domain mapping, which enables us to consider random domains that have large random deviations. This set-up then allows for the reformulation of the problem into an elliptic problem with a random coefficient and a random right-hand side posed on the reference domain. We like to emphasize that the equation obtained on the reference domain no longer corresponds to linear elasticity, but is a vector-valued, uniformly elliptic second order boundary value problem and hence well-posed. Indeed, we may summarize that while the material law is linear and hence the elastic deformations considered should be sufficiently small, the random deformation of the domain itself may be large.

To make the present method feasible for numerical computations, we assume that the random domain mapping is expressed by means of a Karhunen-Loève expansion, following a desired expectation and covariance function. Thus, we can study the regularity of the random solution. It especially turns out that this solution depends analytically on the random input parameters in the Karhunen-Loève expansion. Moreover, the solution's derivatives with respect to the random input parameters may be bounded in terms which are derived from the Karhunen-Loève expansion. These bounds then justify the use of state-of-the-art quadrature methods such as higher-order quasi Monte-Carlo quadratures, e.g. compare [22], or the anisotropic sparse grid Gauss-Legendre quadrature, see [12], to compute deterministic statistics such as the mean or variance of quantities of interest such as the random solution itself or the random von Mises stress as integrals over the countable random input parameters in a dimensionally robust way.

The rest of the article is structured as follows. In Section 2, we model the random boundary value problem under consideration and transform it to the reference domain. The random domain mapping is parameterized by means of the Karhunen-Loève expansion which amounts to a parametric boundary value problem posed on the Cartesian product of reference domain and a countably-dimensional cube. Section 3 presents the regularity analysis of the problem under consideration. These results verify the analytical dependence of the solution on the random input parameters. Numerical studies to validate our findings are performed in Section 4. Finally, the article's conclusion is drawn in Section 5. In addition, some technical lemmata required for the regularity analysis are provided in the appendix.

2. Modelling elasticity problems on random domains.

2.1. Notation. First, we introduce some general notation. Let $D_{\text{ref}} \subset \mathbb{R}^d$, $d = 2, 3$, be a simply connected domain with Lipschitz external boundary Γ_{ref}, which is divided into two subsets Γ_{ref}^D and Γ_{ref}^N satisfying

$$|\Gamma_{\text{ref}}^D|, |\Gamma_{\text{ref}}^N| > 0 \text{ such that } \Gamma_{\text{ref}} = \overline{\Gamma_{\text{ref}}^D} \cup \Gamma_{\text{ref}}^N \text{ and } \Gamma_{\text{ref}}^D \cap \Gamma_{\text{ref}}^N = \emptyset.$$

We assume that the region D_{ref} is an inhomogeneous elastic material, the state of which is given by the vector field of displacements $\boldsymbol{u}(\boldsymbol{x}) = \big(u_1(\boldsymbol{x}), \dots, u_d(\boldsymbol{x})\big)\colon D_{\text{ref}} \to \mathbb{R}^d$. The properties of the material are completely characterized by the fourth order tensor $\mathbb{C}_{\text{ref}}(\boldsymbol{x}) = \{c_{ijkl}(\boldsymbol{x})\}$, where $i, j, k, l = 1, \dots, d$. This material tensor is assumed to satisfies the following symmetry condition

$$c_{ijkl}(\boldsymbol{x}) = c_{jikl}(\boldsymbol{x}) = c_{klij}(\boldsymbol{x}) \quad \text{for all } i, j, k, l = 1, \dots, d,$$

the boundedness condition

$$\sum_{i,j,k,l=1}^{d} c_{klij}(\boldsymbol{x}) \xi_{ij}\, \xi_{kl} \leq C_{\mathbb{C}} |\xi|^2 \quad \text{for all } \underset{\sim}{0} \neq \xi \in \mathbb{R}^{d \times d}, \tag{2.1}$$

and the ellipticity condition

$$\sum_{i,j,k,l=1}^{d} c_{klij}(\boldsymbol{x}) \xi_{ij}\, \xi_{kl} \geq C_{\mathbb{C}}^{-1} |\xi|^2 \quad \text{for all } \underset{\sim}{0} \neq \xi \in \mathbb{R}_{sym}^{d \times d} \tag{2.2}$$

with some constant $C_{\mathbb{C}} \geq 1$ for all $\boldsymbol{x} \in D_{\text{ref}}$. The inhomogeneity of the body under consideration is considered to be piecewise constant, meaning that it can be described by the property

$$\mathbb{C}_{\text{ref}}(\boldsymbol{x}) = \mathbb{C}_0 \mathbb{1}_{D_{\text{ref}} \setminus \cup S_{\text{ref}\,i}}(\boldsymbol{x}) + \sum_{i=1}^{N} \mathbb{C}_i \mathbb{1}_{S_{\text{ref}\,i}}(\boldsymbol{x}).$$

Here, $S_{\text{ref}\,i} \subset D_{\text{ref}}$, $i = 1, \dots, N$, are subdomains with smooth boundaries and $\mathbb{C}_i$, $i = 0, \dots, N$, denote symmetric constant fourth order tensors. Therefore, we also allow for composite materials.

In what follows, we use the following notation for the deformation tensor

$$\varepsilon(\boldsymbol{u}) := \frac{1}{2}\big(\nabla \boldsymbol{u} + (\nabla \boldsymbol{u})^\top\big), \quad \varepsilon_{ij}(\boldsymbol{u}) = \frac{1}{2}\left(\frac{\partial u_i}{\partial x_j} + \frac{\partial u_j}{\partial x_i}\right)$$

and

$$\sigma(\boldsymbol{u}) := \mathbb{C} : \varepsilon(\boldsymbol{u}), \quad \sigma_{ij}(\boldsymbol{u}) = c_{jikl}\, \varepsilon_{kl}(\boldsymbol{u})$$

for the stress tensor.

Throughout the article, we use classical notation for the derivative of a vector-valued function $\boldsymbol{\phi}(\boldsymbol{y}) = \big(\phi_1(y_1, \dots, y_M), \dots, \phi_N(y_1, \dots, y_M)\big)^\top$, that is

$$\partial_{\boldsymbol{y}}^{\boldsymbol{\alpha}} \boldsymbol{\phi} = \left(\frac{\partial^{|\boldsymbol{\alpha}|} \phi_1}{\partial y_1^{\alpha_1} \dots \partial y_M^{\alpha_M}}, \dots, \frac{\partial^{|\boldsymbol{\alpha}|} \phi_N}{\partial y_1^{\alpha_1} \dots \partial y_M^{\alpha_M}}\right)^\top,$$

where $\boldsymbol{\alpha} = (\alpha_1, \dots, \alpha_M) \in \mathbb{N}_0^M$ is a finite multi-index.

2.2. Domain mapping method. Next, we introduce the approach employed to describe an elastic body with random boundary. To this end, consider a complete probability space $(\Omega, \mathcal{F}, \mathbb{P})$ with separable set Ω, σ-field $\mathcal{F} \subset 2^\Omega$ and probability measure $\mathbb{P}$. We then assume that $\boldsymbol{V} : \overline{D_{\text{ref}}} \times \Omega \to \mathbb{R}^d$ is a random vector field such that $\boldsymbol{V}(\cdot, \omega) \in C^1(D_{\text{ref}}; \mathbb{R}^d)$ for almost every $\omega \in \Omega$. It is assumed that there exists some constant $C_{\boldsymbol{V}} > 0$ such that

$$\|\boldsymbol{V}(\cdot,\omega)\|_{C^1(D_{\text{ref}};\mathbb{R}^d)},\ \|\boldsymbol{V}^{-1}(\cdot,\omega)\|_{C^1(D_{\text{ref}};\mathbb{R}^d)} \le C_{\boldsymbol{V}}$$

holds for almost every $\omega \in \Omega$. From this condition, we deduce the property

$$0 < \underline{\lambda} \le \min\{\lambda(\boldsymbol{J})\} \le \max\{\lambda(\boldsymbol{J})\} \le \overline{\lambda} < \infty \tag{2.3}$$

of the singular values $\{\lambda_i\}$ of the Jacobian $\boldsymbol{J} = \nabla \boldsymbol{V}$. Without loss of generality, we assume that $\underline{\lambda} \le 1 \le \overline{\lambda}$. We note that (2.3) especially ensures that almost every realization of the domain transformation $\boldsymbol{V}(D_{\text{ref}}, \omega)$ is a diffeomorphism and hence also bijectiv and bi-Lipschitz.

Having the random vector field $\boldsymbol{V}$ at hand, we can define the random domain under consideration

$$\left.\begin{array}{c} D(\omega) = \boldsymbol{V}(D_{\text{ref}}, \omega), \quad \Gamma(\omega) = \overline{\Gamma^D(\omega)} \cup \Gamma^N(\omega), \\ \Gamma^D(\omega) = \boldsymbol{V}(\Gamma^D_{\text{ref}}, \omega), \quad \Gamma^N(\omega) = \boldsymbol{V}(\Gamma^N_{\text{ref}}, \omega), \\ S_i(\omega) = \boldsymbol{V}(S_{\text{ref}\,i}, \omega) \text{ for all } i = 1, \ldots, N, \end{array}\right\} \quad \omega \in \Omega.$$

Since $\boldsymbol{V}(D_{\text{ref}}, \omega)$ is a diffeomorphism for almost every $\omega \in \Omega$ this also implies that the external boundary $\Gamma(\omega)$ of $D(\omega)$ necessarily is a Lipschitz boundary for almost every $\omega \in \Omega$. We also define the respective hold-all

$$\mathcal{D} = \bigcup_{\omega \in \Omega} D(\omega), \quad \mathcal{G}^D = \bigcup_{\omega \in \Omega} \Gamma^D(\omega) \quad \text{and} \quad \mathcal{G}^N = \bigcup_{\omega \in \Omega} \Gamma^N(\omega).$$

We are now in the position to state the equilibrium problem of the elastic body with a random boundary which we will study in the rest of this article:

$$\begin{gathered} \text{for given } \boldsymbol{f}(\boldsymbol{x}) \in H^{-1}(\mathcal{D})^d,\ \boldsymbol{g}(\boldsymbol{x}) \in H^{-1/2}(\mathcal{G}^N)^d \text{ and } \boldsymbol{V}(\boldsymbol{x}, \omega) \\ \text{find } \boldsymbol{u}(\boldsymbol{x}, \omega) \in H^1\big(D(\omega)\big)^d \text{ satisfying} \\ -\operatorname{div}\big(\sigma(\boldsymbol{u}(\boldsymbol{x}, \omega)\big) = \boldsymbol{f}(\boldsymbol{x}) \text{ in } D(\omega), \\ \boldsymbol{u}(\boldsymbol{x}, \omega) = \boldsymbol{0} \text{ on } \Gamma^D(\omega), \\ \sigma\big(\boldsymbol{u}(\boldsymbol{x}, \omega)\big)\boldsymbol{n}(\omega) = \boldsymbol{g}(\boldsymbol{x}) \text{ on } \Gamma^N(\omega). \end{gathered}$$

Here, $\boldsymbol{n}(\omega)$ denotes the unit exterior normal at the domain's boundary $\Gamma(\omega)$ and $\sigma\big(\boldsymbol{u}(\boldsymbol{x}, \omega)\big) = \mathbb{C}(\boldsymbol{x}, \omega) : \varepsilon\big(\boldsymbol{u}(\boldsymbol{x}, \omega)\big)$. In case of composite materials, we especially have

$$\mathbb{C}(\boldsymbol{x}, \boldsymbol{w}) = \mathbb{C}_0 \mathbb{1}_{D(\omega) \setminus \cup S_i(\omega)}(\boldsymbol{x}) + \sum_{i=1}^N \mathbb{C}_i \mathbb{1}_{S_i(\omega)}(\boldsymbol{x}).$$

Note that the above formulation of linear elasticity is known as the displacement or primal formulation.

To derive the variational formulation, let us define the set of admissible solutions

$$\mathcal{H}\big(D(\omega)\big) = \big\{\boldsymbol{v}(\boldsymbol{x},\omega) \in H^1\big(D(\omega)^d\big) \,\big|\, \boldsymbol{v}(\boldsymbol{x}) = 0 \text{ on } \Gamma^D(\omega)\big\}.$$

Then, we reformulate the above boundary value problem in accordance with the variational formulation:

$$\text{(2.4)} \qquad \left\{\begin{aligned} &\text{for given } \boldsymbol{f}(\boldsymbol{x}) \in H^{-1}(\mathcal{D})^d,\ \boldsymbol{g}(\boldsymbol{x}) \in H^{-1/2}(\mathcal{G}^N)^d \text{ and } \boldsymbol{V}(\boldsymbol{x},\omega) \\ &\qquad \text{find } \boldsymbol{u}(\boldsymbol{x},\omega) \in \mathcal{H}\big(D(\omega)\big) \text{ such that} \\ &\int_{D(\omega)} \sigma\big(\boldsymbol{u}(\boldsymbol{x},\omega)\big) : \varepsilon(\boldsymbol{v}(\boldsymbol{x},\omega))\,\mathrm{d}\boldsymbol{x} = \int_{D(\omega)} \boldsymbol{f}(\boldsymbol{x}) \cdot \boldsymbol{v}(\boldsymbol{x},\omega)\,\mathrm{d}\boldsymbol{x} \\ &\quad + \int_{\Gamma^N(\omega)} \boldsymbol{g}(\boldsymbol{x}) \cdot \boldsymbol{v}(\boldsymbol{x},\omega)\,\mathrm{d}\boldsymbol{s} \text{ for all } \boldsymbol{v}(\boldsymbol{x},\omega) \in \mathcal{H}\big(D(\omega)\big). \end{aligned}\right.$$

As is widely known, for almost every fixed ω this problem has a unique solution, compare [2, 5] for example.

In our setting, it is more convenient to reformulate problem (2.4) on the deterministic reference domain D_{ref} but with random coefficients $\mathbb{C}(\boldsymbol{x},\omega)$. Especially, for such problems, there are already many different methods available to solve them. The main tool we use here is the one-to-one correspondence between the problem on random domain $D(\omega)$ and the problem with random coefficients on the deterministic reference domain D_{ref} due to the random domain mapping. So, for an arbitrary vector field $\boldsymbol{v}$ on $D(\omega)$, we denote the transported field by $\hat{\boldsymbol{v}}(\boldsymbol{x},\omega) := (\boldsymbol{v} \circ \boldsymbol{V})(\boldsymbol{x},\omega)$. According to the chain rule, it is easy to formulate the problem for $\boldsymbol{v}$ by pulling the original problem back onto D_{ref}.

To this end, we first introduce the new set of admissible solutions

$$\mathcal{H}(D_{\text{ref}}) = \big\{\boldsymbol{v}(\boldsymbol{x}) \in H^1(D_{\text{ref}})^d \,\big|\, \boldsymbol{v}(\boldsymbol{x}) = 0 \text{ on } \Gamma^D_{\text{ref}}\big\}.$$

The connection between $\mathcal{H}(D_{\text{ref}})$ and $\mathcal{H}\big(D(\omega)\big)$ is described by the following lemma.

Lemma 2.1. *The spaces $\mathcal{H}(D_{\text{ref}})$ and $\mathcal{H}\big(D(\omega)\big)$ are isomorphic by means of the isomorphism*

$$\mathcal{V} : \mathcal{H}(D_{\text{ref}}) \to H\big(D(\omega)\big), \quad \boldsymbol{v} \mapsto \boldsymbol{v} \circ \boldsymbol{V}^{-1}(\omega).$$

Proof. The proof is a consequence of the ellipticity assumption (2.3). ■

This lemma thus implies that

$$\mathcal{H}\big(D(\omega)\big) = \big\{\boldsymbol{v} = \mathcal{V}(\hat{\boldsymbol{v}}) \,\big|\, \hat{\boldsymbol{v}} \in \mathcal{H}(D_{\text{ref}})\big\}.$$

Thus, for an arbitrary function $\mathcal{V}(\hat{\boldsymbol{v}}) \in \mathcal{H}\big(D(\omega)\big)$, there holds

$$\widehat{\mathcal{V}(\hat{\boldsymbol{v}})} = \mathcal{V}(\hat{\boldsymbol{v}}) \circ \boldsymbol{V} = \hat{\boldsymbol{v}} \circ \boldsymbol{V}^{-1} \circ \boldsymbol{V} = \hat{\boldsymbol{v}} \in \mathcal{H}(D_{\text{ref}}).$$

This allows us to consider the test functions $\hat{\boldsymbol{v}}$ to be independent of ω. Moreover, by using the symmetry of $\mathbb{C}_{\text{ref}}$, we deduce

$$\sigma(\boldsymbol{u}) = \mathbb{C}_{\text{ref}} : \varepsilon(\boldsymbol{u}) = \mathbb{C}_{\text{ref}} : \nabla\boldsymbol{u}.$$

Therefore, by pulling back in (2.4), we get the following formulation:

$$
\begin{cases}
\text{for given } \boldsymbol{f}(\boldsymbol{x}) \in H^{-1}(\mathcal{D}),\ \boldsymbol{g}(\boldsymbol{x}) \in H^{-1/2}(\mathcal{G}^N) \text{ and } \boldsymbol{V}(\boldsymbol{x},\omega) \\
\text{find } \hat{\boldsymbol{u}}(\boldsymbol{x},\omega) \in \mathcal{H}(D_{\mathrm{ref}}) \text{ such that} \\
\displaystyle\int_{D_{\mathrm{ref}}} \widetilde{\mathbb{C}}(\boldsymbol{x},\omega) : \nabla\hat{\boldsymbol{u}}(\boldsymbol{x},\omega) : \nabla\hat{\boldsymbol{v}}(\boldsymbol{x}) \,\mathrm{d}\boldsymbol{x} = \int_{D_{\mathrm{ref}}} \widetilde{\boldsymbol{f}}(\boldsymbol{x},\omega) \cdot \hat{\boldsymbol{v}}(\boldsymbol{x}) \,\mathrm{d}\boldsymbol{x} \\
\qquad + \displaystyle\int_{\Gamma^N_{\mathrm{ref}}} \widetilde{\boldsymbol{g}}(\boldsymbol{x}) \cdot \boldsymbol{v}(\boldsymbol{x},\omega) \,\mathrm{d}\boldsymbol{s} \text{ for all } \hat{\boldsymbol{v}}(\boldsymbol{x}) \in \hat{\boldsymbol{v}}(\boldsymbol{x}) \in \mathcal{H}(D_{\mathrm{ref}}).
\end{cases}
\tag{2.5}
$$

Here, we have

$$
\begin{gathered}
\widetilde{\boldsymbol{f}}(\boldsymbol{x},\omega) = \det \boldsymbol{J}(\boldsymbol{x},\omega)\hat{\boldsymbol{f}}(\boldsymbol{x},\omega), \quad \widetilde{\boldsymbol{g}}(\boldsymbol{x},\omega) = \kappa(\boldsymbol{x},\omega) \det \boldsymbol{J}(\boldsymbol{x},\omega)\hat{\boldsymbol{g}}(\boldsymbol{x},\omega), \\
\kappa(\boldsymbol{x},\omega) = \big\| \boldsymbol{J}^{-\top}(\boldsymbol{x},\omega)\boldsymbol{n}_{\mathrm{ref}}(\boldsymbol{x}) \big\|, \\
\widetilde{\mathbb{C}}(\boldsymbol{x},\omega) = \det \boldsymbol{J}(\boldsymbol{x},\omega)\boldsymbol{J}^{-1}(\boldsymbol{x},\omega)\mathbb{C}_{\mathrm{ref}}(\boldsymbol{x})\boldsymbol{J}^{-\top}(\boldsymbol{x},\omega).
\end{gathered}
\tag{2.6}
$$

Note that the solution of the initial problem (2.4) can be simply reconstructed from the solution of (2.5) by $u(\boldsymbol{x},\omega) = (\hat{u} \circ \boldsymbol{V}^{-1})(\boldsymbol{x},\omega)$ with $\boldsymbol{x} \in D(\omega)$.

Remark 2.2. The problem can be rewritten differently, using another formulation for the pulled back stress and deformation tensors. Namely, we have

$$
\begin{aligned}
\widetilde{\sigma}(\hat{\boldsymbol{u}}(\boldsymbol{x},\omega)) &= \mathbb{C}_{\mathrm{ref}} : \widetilde{\varepsilon}(\hat{\boldsymbol{u}}(\boldsymbol{x},\omega)) \\
&= \mathbb{C}_{\mathrm{ref}} : \frac{1}{2}\Big(\boldsymbol{J}^{-\top}(\boldsymbol{x},\omega)\nabla\hat{\boldsymbol{u}}(\boldsymbol{x},\omega) + \nabla\hat{\boldsymbol{u}}^{\top}(\boldsymbol{x},\omega)\boldsymbol{J}^{-1}(\boldsymbol{x},\omega)\Big),
\end{aligned}
$$

The advantage of this formulation is that it preserves symmetry, which means that one directly has the ellipticity property. However, the formulation is inconvenient to work with when one is concerned with the regularity of the solution as a function of the random input parameterts. Moreover, another more general notation by the elastic potential W is common to describe the deformation of a solid body, i.e. $\sigma(\boldsymbol{u}) = W(\nabla\boldsymbol{u})$. In our case, there holds $W(\nabla\hat{\boldsymbol{u}}(\boldsymbol{x},\omega))) = \widetilde{\mathbb{C}}(\boldsymbol{x},\omega) : \nabla\hat{\boldsymbol{u}}(\boldsymbol{x},\omega)$, i.e. we can say that we are considering deformation of some nonhomogeneous solid.

Remark 2.3. Since $\boldsymbol{V}$ is assumed to be a C^1-diffeomorphism, we have that $\det(\boldsymbol{J}) \neq 0$. Therefore, without loss of generality, we may assume the positiveness of the determinant in (2.6).

2.3. Karhunen-Loève expansion. We next define the framework in which we model the uncertainty. We assume that the vector field $\boldsymbol{V}(\boldsymbol{x},\omega) = \big(V_1(\boldsymbol{x},\omega),\dots,V_d(\boldsymbol{x},\omega)\big)^{\top} : \Omega \to \mathcal{B}$ belongs to the Lebesgue-Bochner space $L^p_{\mathbb{P}}(\Omega;\mathcal{B})$ with norm

$$
\|\boldsymbol{V}\|_{L^p_{\mathbb{P}}(\Omega;\mathcal{B})} := \begin{cases} \left(\displaystyle\int_{\Omega} \|\boldsymbol{V}\|^p_{\mathcal{B}} \,\mathrm{d}\mathbb{P}(\omega)\right)^{1/p}, & p < \infty, \\ \operatorname*{ess\,sup}_{\omega\in\Omega} \|\boldsymbol{V}\|_{\mathcal{B}}\,, & p = \infty. \end{cases}
$$

The mean of $\boldsymbol{V}$ is given by $\mathbb{E}[\boldsymbol{V}](\boldsymbol{x}) = \big(\mathbb{E}[V_1](\boldsymbol{x}), \dots, \mathbb{E}[V_d](\boldsymbol{x})\big)^\top$, where

$$\mathbb{E}[V_i](\boldsymbol{x}) := \int_\Omega V_i(\boldsymbol{x}, \omega) \,\mathrm{d}\mathbb{P}(\omega), \quad i = 1, \dots, d.$$

The matrix-valued covariance function $\mathrm{Cov}[\boldsymbol{V}](\boldsymbol{x}, \boldsymbol{y})$ is given by

$$\mathrm{Cov}_{ij}[\boldsymbol{V}](\boldsymbol{x}, \boldsymbol{y}) = \mathbb{E}\Big[\big(V_i(\boldsymbol{x}, \omega) - \mathbb{E}[V_i](\boldsymbol{x})\big)\big(V_j(\boldsymbol{y}, \omega) - \mathbb{E}[V_j](\boldsymbol{y})\big)\Big], \quad i, j = 1, \dots, d.$$

Next, we introduce the integral operator $\mathcal{S}_{\boldsymbol{V}} : L^2_{\mathbb{P}}(\Omega) \to L^2(D_{\mathrm{ref}}; \mathbb{R}^d)$ defined by

$$\mathcal{S}_{\boldsymbol{V}}\langle X\rangle(\boldsymbol{x}) := \int_\Omega \big(\boldsymbol{V}(\boldsymbol{x}, \omega) - \mathbb{E}[\boldsymbol{V}](\boldsymbol{x})\big) X(\omega) \,\mathrm{d}\mathbb{P}(\omega).$$

Its adjoint $\mathcal{S}^*_{\boldsymbol{V}} : L^2(D_{\mathrm{ref}}; \mathbb{R}^d) \to L^2_{\mathbb{P}}(\Omega)$ reads as

$$\mathcal{S}^*_{\boldsymbol{V}}\langle \boldsymbol{v}\rangle(\boldsymbol{x}) := \int_{D_{\mathrm{ref}}} \big(\boldsymbol{V}(\boldsymbol{x}, \omega) - \mathbb{E}[\boldsymbol{V}](x)\big)^\top \boldsymbol{v}(\boldsymbol{x}) \,\mathrm{d}\boldsymbol{x}.$$

With the help of these operators, the covariance operator $\mathcal{C}_{\boldsymbol{V}} : L^2(D_{\mathrm{ref}}; \mathbb{R}^d) \to L^2(D_{\mathrm{ref}}; \mathbb{R}^d)$ associated with the random field $\boldsymbol{V}(\boldsymbol{x}, \omega)$ is given by

$$\mathcal{C}_{\boldsymbol{V}}\langle \boldsymbol{v}\rangle(\boldsymbol{x}) := S_{\boldsymbol{V}}\big\langle S^*_{\boldsymbol{V}}\langle \boldsymbol{v}\rangle\big\rangle(\boldsymbol{x}) = \int_{D_{\mathrm{ref}}} \mathrm{Cov}[\boldsymbol{V}](\boldsymbol{x}, \boldsymbol{y}) \boldsymbol{v}(\boldsymbol{y}) \,\mathrm{d}\boldsymbol{y}. \tag{2.7}$$

According to [1], the covariance operator (2.7) satisfies the following statement.

Theorem 2.4. *Let $\mathcal{C}_{\boldsymbol{V}} : L^2(D_{\mathrm{ref}}; \mathbb{R}^d) \to L^2(D_{\mathrm{ref}}; \mathbb{R}^d)$ be the covariance operator (2.7) related to the random field $\boldsymbol{V}(\boldsymbol{x}, \omega) \in L^2_{\mathbb{P}}\big(\Omega; L^2(D_{\mathrm{ref}}; \mathbb{R}^d)\big)$. Then, there exist a sequence $\{\boldsymbol{\phi}_k\}$ of orthonormal eigenfunctions and a null sequence $\lambda_1 \geq \lambda_2 \geq \cdots \geq 0$ of eigenvalues satisfying*

$$\mathcal{C}_{\boldsymbol{V}}\langle \boldsymbol{\phi}_k\rangle = \lambda_k \boldsymbol{\phi}_k \quad \textit{for all} \quad k = 1, 2, \dots.$$

Furthermore, there holds

$$\mathcal{C}_{\boldsymbol{V}}\langle \boldsymbol{v}\rangle = \sum_{k=1}^\infty \lambda_k \langle \boldsymbol{v}, \boldsymbol{\phi}_k\rangle_{L^2(D_{\mathrm{ref}};\mathbb{R}^d)} \boldsymbol{\phi}_k \quad \textit{for all} \quad \boldsymbol{v} \in L^2(D_{\mathrm{ref}}; \mathbb{R}^d),$$

where $\langle \boldsymbol{v}, \boldsymbol{u}\rangle_{L^2(D_{\mathrm{ref}};\mathbb{R}^d)}$ is the inner product in $L^2(D_{\mathrm{ref}}; \mathbb{R}^d)$.

Theorem 2.4 implies that we can expand the random vector field $\boldsymbol{V}(\boldsymbol{x}, \omega)$ as the Karhunen-Loève expansion

$$\boldsymbol{V}(\boldsymbol{x}, \omega) = \mathbb{E}[\boldsymbol{V}](\boldsymbol{x}) + \sum_{k=1}^\infty \sqrt{\lambda_k} \boldsymbol{\phi}_k(\boldsymbol{x}) X_k(\omega),$$

where $X_k(\omega) = \frac{1}{\sqrt{\lambda_k}} \mathcal{S}^*_{\boldsymbol{V}}\langle \boldsymbol{\phi}_k\rangle(\omega)$ are normalized and uncorrelated random variables.

We consider the random vector field $\boldsymbol{V}$ to map Ω into the Sobolev space $H^p(D_{\mathrm{ref}}, \mathbb{R}^d)$. Then, from [10, 11], we get the following result.

Theorem 2.5. *The eigenvalues of the covariance operator $\mathcal{C}_{\boldsymbol{V}}$ satisfy $\lambda_k = \mathcal{O}(k^{-(2\frac{p}{d}+1)})$ provided that $\boldsymbol{V} \in L^2_{\mathbb{P}}\big(\Omega;\, H^p(D_{\mathrm{ref}};\, \mathbb{R}^d)\big)$.*

In the rest of the article, we will assume that

- the random variables $\{X_k\}$ are independent and uniformly distributed in $[-\sqrt{3}, \sqrt{3}]$;
- the sequence $\{\gamma_k\} := \big\{\|2\sqrt{3\lambda_k}\boldsymbol{\phi}_k\|_{W^{1,\infty}(D_{\mathrm{ref}};\mathbb{R}^d)}\big\}$ is at least in $\ell^1(\mathbb{N})$;
- the mean satisfies $\mathbb{E}[\boldsymbol{V}](\boldsymbol{x}) = \boldsymbol{x}$.

These model assumptions imply that the random domain mapping $\boldsymbol{V}(\boldsymbol{x}, \omega)$ belongs to the Bochner space $L^\infty_{\mathbb{P}}\big(\Omega;\, W^{1,\infty}(D_{\mathrm{ref}};\, \mathbb{R}^d)\big)$. Moreover, they allow for truncation of the Karhunen-Loève expansion for some $0 < M < \infty$ and then parametrize it to arrive at

$$\boldsymbol{V}(\boldsymbol{x}, \boldsymbol{y}) = \boldsymbol{x} + \sum_{k=1}^{M} 2\sqrt{3\lambda_k}\boldsymbol{\phi}_k(\boldsymbol{x})y_k, \quad \boldsymbol{y} = (y_1, \ldots, y_M) \in \square := [-1/2, 1/2]^M. \tag{2.8}$$

Note that $L^\infty(\square)$ is equipped with the push-forward measure $\mathbb{P}_{\boldsymbol{X}} = \mathbb{P} \circ \boldsymbol{X}^{-1}$, where $\boldsymbol{X}(\omega) = \big(X_1(\omega), \ldots, X_M(\omega)\big)$ consists of the random variables under consideration.

Remark 2.6. We model the random vector field here by means of the Karhunen-Loève expansion, prescribing its expectation and covariance kernel. Nonetheless, our theory applies for any affine expansion of the random vector field in the form (2.8), too.

2.4. Problem statement. We are now in the position to formulate the full problem which we will consider in the rest part of the work:

$$\left\{\begin{aligned} &\text{for given } \boldsymbol{f}(\boldsymbol{x}) \in H^{-1}(\mathcal{D}),\ \boldsymbol{g}(\boldsymbol{x}) \in H^{-1/2}(\mathcal{G}^N) \text{ and } \boldsymbol{V}(\boldsymbol{x}, \boldsymbol{y}) \text{ as in (2.8)} \\ &\qquad\qquad \text{find } \hat{\boldsymbol{u}}(\boldsymbol{x}, \boldsymbol{y}) \in \mathcal{H}(D_{\mathrm{ref}}) \text{ such that} \\ &\int_{D_{\mathrm{ref}}} \widetilde{\mathbb{C}}(\boldsymbol{x}, \boldsymbol{y}) : \nabla\hat{\boldsymbol{u}}(\boldsymbol{x}, \boldsymbol{y}) : \nabla\hat{\boldsymbol{v}}(\boldsymbol{x})\,\mathrm{d}\boldsymbol{x} = \int_{D_{\mathrm{ref}}} \widetilde{\boldsymbol{f}}(\boldsymbol{x}, \boldsymbol{y}) \cdot \hat{\boldsymbol{v}}(\boldsymbol{x})\,\mathrm{d}\boldsymbol{x} \\ &\qquad + \int_{\Gamma^N_{\mathrm{ref}}} \widetilde{\boldsymbol{g}}(\boldsymbol{x}) \cdot \boldsymbol{v}(\boldsymbol{x}, \boldsymbol{y})\,\mathrm{d}\boldsymbol{s} \text{ for all } \hat{\boldsymbol{v}}(\boldsymbol{x}) \in \hat{\boldsymbol{v}}(\boldsymbol{x}) \in \mathcal{H}(D_{\mathrm{ref}}), \end{aligned}\right. \tag{2.9}$$

where $\widetilde{\mathbb{C}}$, $\widetilde{f}$ and $\widetilde{g}$ are defined as in (2.6).

Lemma 2.7. *The bilinear form appearing in* (2.9) *is coercive with bound*

$$\langle\widetilde{\mathbb{C}} : \nabla\hat{\boldsymbol{v}}, \nabla\hat{\boldsymbol{v}}\rangle_{L^2(D_{\mathrm{ref}};\mathbb{R}^2)} \geq \frac{C_{\mathbb{C}}^{-1}}{2}\frac{\underline{\lambda}^d}{\overline{\lambda}^2}\|\hat{\boldsymbol{v}}\|^2_{H^1(D_{\mathrm{ref}})},$$

where

$$\langle\widetilde{\mathbb{C}} : \nabla\hat{\boldsymbol{v}}, \nabla\hat{\boldsymbol{v}}\rangle_{L^2(D_{\mathrm{ref}};\mathbb{R}^2)} = \int_{D_{\mathrm{ref}}} \widetilde{\mathbb{C}}(\boldsymbol{x}, \boldsymbol{y}) : \nabla\hat{\boldsymbol{u}}(\boldsymbol{x}, \boldsymbol{y}) : \nabla\hat{\boldsymbol{v}}(\boldsymbol{x})\, d\boldsymbol{x}.$$

Proof. Using Korn's inequality and the ellipticity conditions (2.2) resp. (2.3), we conclude the coercivity of the following bilinear form as follows:

$$\begin{aligned} \langle\widetilde{\mathbb{C}} : \nabla\hat{\boldsymbol{v}}, \nabla\hat{\boldsymbol{v}}\rangle_{L^2(D_{\mathrm{ref}};\mathbb{R}^2)} &= \langle\mathbb{C} : \nabla\boldsymbol{v}, \nabla\boldsymbol{v}\rangle_{L^2(D(\omega);\mathbb{R}^2)} = \int_{D(\omega)} \sigma\big(\boldsymbol{v}(\boldsymbol{x}, \omega)\big) : \varepsilon\big(\boldsymbol{v}(\boldsymbol{x}, \omega)\big)\,\mathrm{d}\boldsymbol{x} \\ &\geq C_{\mathbb{C}}^{-1}\int_{D(\omega)} \varepsilon\big(\boldsymbol{v}(\boldsymbol{x}, \omega)\big) : \varepsilon\big(\boldsymbol{v}(\boldsymbol{x}, \omega)\big)\,\mathrm{d}\boldsymbol{x} \geq \frac{C_{\mathbb{C}}^{-1}}{2}\|\boldsymbol{v}\|^2_{H^1(D(\omega)} \geq \frac{C_{\mathbb{C}}^{-1}}{2}\frac{\underline{\lambda}^d}{\overline{\lambda}^2}\|\hat{\boldsymbol{v}}\|^2_{H^1(D_{\mathrm{ref}})}. \end{aligned}$$

∎

The following result is an immediate consequence of the previous lemma.

Corollary 2.8. *The problem* (2.9) *has a unique solution which satisfies*

$$\|\hat{\boldsymbol{u}}\|_{H^1(D_{\mathrm{ref}})} \leq 2C_{\mathbb{C}} \frac{\overline{\lambda}^2}{\underline{\lambda}^d} \Big(\|\widetilde{\boldsymbol{f}}\|_{L^\infty(\square;H^{-1}(D_{\mathrm{ref}}))} + \|\widetilde{\boldsymbol{g}}\|_{L^\infty(\square;H^{-1/2}(\Gamma^N_{\mathrm{ref}}))} \Big).$$

3. Parametric regularity of the solution. In this section, we study the regularity of the solution $\boldsymbol{u}(\boldsymbol{x},\boldsymbol{y})$ of the problem (2.5) with respect to random domains related to $\boldsymbol{V}(\boldsymbol{x},\boldsymbol{y})$ from (2.8). To this end, we assume that the body force $\boldsymbol{f}(\boldsymbol{x})$ and the external surface force $\boldsymbol{g}(\boldsymbol{x})$ are analytic functions. Moreover, we define the space $L^\infty\big(\square; L^\infty(D_{\mathrm{ref}}; \mathbb{R}^d \times \mathbb{R}^d)\big)$, which consists of all equivalence classes of strongly measurable functions $A : \square \to L^\infty(D_{\mathrm{ref}}; \mathbb{R}^d \times \mathbb{R}^d)$ with finite norm

$$\|\!|A|\!\|_\infty := \operatorname*{ess\,sup}_{\boldsymbol{y}\in\square} \|A(\boldsymbol{y})\|_{L^\infty(D_{\mathrm{ref}};\mathbb{R}^d\times\mathbb{R}^d)}. \tag{3.1}$$

Our main result is then formulated in the following theorem.

Theorem 3.1. *Let* $\hat{\mathbf{u}}(\boldsymbol{x},\boldsymbol{y})$ *be the solution to* (2.9) *under the aforementioned assumptions. Then, for* $\boldsymbol{V}$ *defined by* (2.8)*, there exist constants* C_1, C_2 *such that*

$$\|\partial_{\boldsymbol{y}}^{\boldsymbol{\alpha}} \hat{\mathbf{u}}\|_{H^1(D_{\mathrm{ref}})} \leq C_1^{|\boldsymbol{\alpha}|+1} |\boldsymbol{\alpha}|! \boldsymbol{\mu}^{\boldsymbol{\alpha}}, \quad \text{where} \quad \boldsymbol{\mu} = (C_2\gamma_1, \ldots, C_2\gamma_M).$$

Proof. The proof of this theorem is based on the technical lemmata given in the appendix and formally repeats ideas from [15].

Differentiating the variational formulation (2.9) with respect to $\boldsymbol{y}$ and applying the Leibniz rule gives us

$$\int_{D_{\mathrm{ref}}} \sum_{\boldsymbol{\alpha}'\leq\boldsymbol{\alpha}} \binom{\boldsymbol{\alpha}}{\boldsymbol{\alpha}'} \partial_{\boldsymbol{y}}^{\boldsymbol{\alpha}'} \tilde{\mathbb{C}}(\boldsymbol{x},\boldsymbol{y}) : \partial_{\boldsymbol{y}}^{\boldsymbol{\alpha}-\boldsymbol{\alpha}'} \nabla \hat{\boldsymbol{u}}(\boldsymbol{x},\boldsymbol{y}) : \nabla \hat{\boldsymbol{v}}(\boldsymbol{x}) \,\mathrm{d}\boldsymbol{x}$$
$$= \int_{D_{\mathrm{ref}}} \partial_{\boldsymbol{y}}^{\boldsymbol{\alpha}} \tilde{\boldsymbol{f}}(\boldsymbol{x},\boldsymbol{y}) \cdot \hat{\boldsymbol{v}}(\boldsymbol{x}) \,\mathrm{d}\boldsymbol{x} + \int_{\Gamma^N_{\mathrm{ref}}} \partial_{\boldsymbol{y}}^{\boldsymbol{\alpha}} \tilde{\boldsymbol{g}}(\boldsymbol{x},\boldsymbol{y}) \cdot \hat{\boldsymbol{v}}(\boldsymbol{x}) \,\mathrm{d}\boldsymbol{s}.$$

We rearrange the preceding expression which leads to

$$\begin{aligned} \int_{D_{\mathrm{ref}}} \tilde{\mathbb{C}}(\boldsymbol{x},\boldsymbol{y}) : \partial_{\boldsymbol{y}}^{\boldsymbol{\alpha}} \nabla \hat{\boldsymbol{u}}(\boldsymbol{x},\boldsymbol{y}) : \nabla \hat{\boldsymbol{v}}(\boldsymbol{x}) \,\mathrm{d}\boldsymbol{x} &= \int_{D_{\mathrm{ref}}} \partial_{\boldsymbol{y}}^{\boldsymbol{\alpha}} \tilde{\boldsymbol{f}}(\boldsymbol{x},\boldsymbol{y}) \cdot \hat{\boldsymbol{v}}(\boldsymbol{x}) \,\mathrm{d}\boldsymbol{x} \\ + \int_{\Gamma^N_{\mathrm{ref}}} \partial_{\boldsymbol{y}}^{\boldsymbol{\alpha}} \tilde{\boldsymbol{g}}(\boldsymbol{x},\boldsymbol{y}) \cdot \hat{\boldsymbol{v}}(\boldsymbol{x}) \,\mathrm{d}\boldsymbol{s} &- \int_{D_{\mathrm{ref}}} \sum_{\boldsymbol{\alpha}'<\boldsymbol{\alpha}} \binom{\boldsymbol{\alpha}}{\boldsymbol{\alpha}'} \partial_{\boldsymbol{y}}^{\boldsymbol{\alpha}-\boldsymbol{\alpha}'} \tilde{\mathbb{C}}(\boldsymbol{x},\boldsymbol{y}) : \partial_{\boldsymbol{y}}^{\boldsymbol{\alpha}'} \nabla \hat{\boldsymbol{u}}(\boldsymbol{x},\boldsymbol{y}) : \nabla \hat{\boldsymbol{v}}(\boldsymbol{x}) \,\mathrm{d}\boldsymbol{x}. \end{aligned} \tag{3.2}$$

Applying the Leibniz rule again and using (2.1), we conclude

$$\int_{D_{\mathrm{ref}}} \partial_{\boldsymbol{y}}^{\boldsymbol{\alpha}} \tilde{\mathbb{C}} : \nabla \hat{\boldsymbol{u}} : \nabla \hat{\boldsymbol{u}} \,\mathrm{d}\boldsymbol{x} \leq C_{\mathbb{C}} \big\|\!\big| \partial_{\boldsymbol{y}}^{\boldsymbol{\alpha}} A \big|\!\big\|_\infty \|\hat{u}\|^2_{H^1(D_{\mathrm{ref}})}, \tag{3.3}$$

where

$$A(\boldsymbol{x},\boldsymbol{y}) = \det \boldsymbol{J}(\boldsymbol{x},\boldsymbol{y}) \big(\boldsymbol{J}^\top(\boldsymbol{x},\boldsymbol{y}) \boldsymbol{J}(\boldsymbol{x},\boldsymbol{y})\big)^{-1}.$$

Next, we simplify the estimates formulated in the lemmas in the appendix. We first note that for all $\boldsymbol{f} \in L^\infty\big(\square; H^{-1}(D_{\mathrm{ref}})\big)$ and $\boldsymbol{g} \in L^\infty\big(\square; H^{-1/2}(\Gamma_{\mathrm{ref}}^N)\big)$ the norm estimates

$$\begin{aligned} \|\boldsymbol{f}\|_{L^\infty(\square;H^{-1}(D_{\mathrm{ref}}))} &\leq C_D \|\boldsymbol{f}\|_{L^\infty(\square;L^\infty(D_{\mathrm{ref}}))}, \\ \|\boldsymbol{g}\|_{L^\infty(\square;H^{-1/2}(\Gamma_{\mathrm{ref}}^N))} &\leq C_\Gamma \|\boldsymbol{g}\|_{L^\infty(\square;L^\infty(\Gamma_{\mathrm{ref}}^N))} \end{aligned} \tag{3.4}$$

hold, where C_D and C_Γ depend only on D_{ref} and Γ_{ref}^N, respectively. Taking

$$C' = C_{\mathrm{det}} \max\left\{\frac{1}{\underline{\lambda}^2}, C_f, \frac{C_g}{2\underline{\lambda}}\right\}, \quad C'' = 6 \max\left\{\frac{2(1+C_{\boldsymbol{\gamma}})}{\underline{\lambda}^2 \log 2}, \frac{d}{\rho_f \log 2}, \frac{d}{\underline{\lambda}\rho_g (\log 2)^2}\right\},$$

and

$$\boldsymbol{\mu} = (C''\gamma_1, \ldots, C''\gamma_M)$$

for $|\boldsymbol{\alpha}| > 0$, using (3.4) we can hence reformulate (A.1), (A.2) and (A.3) as

$$\begin{aligned} \big|\big|\big|\partial_{\boldsymbol{y}}^{\boldsymbol{\alpha}} A\big|\big|\big|_\infty &\leq C'|\boldsymbol{\alpha}|!\boldsymbol{\mu}^{\boldsymbol{\alpha}}, \\ \|\partial_{\boldsymbol{y}}^{\boldsymbol{\alpha}} \widetilde{\boldsymbol{f}}\|_{L^\infty(\square;H^{-1}(D_{\mathrm{ref}}))} &\leq C_D C'|\boldsymbol{\alpha}|!\boldsymbol{\mu}^{\boldsymbol{\alpha}}, \\ \|\partial_{\boldsymbol{y}}^{\boldsymbol{\alpha}} \widetilde{\boldsymbol{g}}\|_{L^\infty(\square;H^{-1/2}(\Gamma_{\mathrm{ref}}^N))} &\leq C_\Gamma C'|\boldsymbol{\alpha}|!\boldsymbol{\mu}^{\boldsymbol{\alpha}}. \end{aligned} \tag{3.5}$$

We choose $\hat{\boldsymbol{v}} = \partial_{\boldsymbol{y}}^{\boldsymbol{\alpha}} \hat{\boldsymbol{u}}$ in (3.2) and employ the estimates (3.3), (3.5), and Lemma 2.7 to arrive at

$$\begin{aligned} &\frac{C_{\mathbb{C}}^{-1}}{2}\frac{\underline{\lambda}^d}{\overline{\lambda}^2}\|\partial_{\boldsymbol{y}}^{\boldsymbol{\alpha}} \hat{\boldsymbol{u}}\|_{H^1(D_{\mathrm{ref}})}^2 \leq C'(C_D + C_\Gamma)|\boldsymbol{\alpha}|!\boldsymbol{\mu}^{\boldsymbol{\alpha}} \|\partial_{\boldsymbol{y}}^{\boldsymbol{\alpha}} \hat{\boldsymbol{u}}\|_{H^1(D_{\mathrm{ref}})} \\ &+ C' C_{\mathbb{C}} \sum_{\boldsymbol{\alpha}' < \boldsymbol{\alpha}} \binom{\boldsymbol{\alpha}}{\boldsymbol{\alpha}'} |\boldsymbol{\alpha} - \boldsymbol{\alpha}'|! \boldsymbol{\mu}^{\boldsymbol{\alpha}-\boldsymbol{\alpha}'} \|\partial_{\boldsymbol{y}}^{\boldsymbol{\alpha}'} \hat{\boldsymbol{u}}\|_{H^1(D_{\mathrm{ref}})} \|\partial_{\boldsymbol{y}}^{\boldsymbol{\alpha}} \hat{\boldsymbol{u}}\|_{H^1(D_{\mathrm{ref}})}. \end{aligned}$$

From this we obtain

$$\|\partial_{\boldsymbol{y}}^{\boldsymbol{\alpha}} \hat{\boldsymbol{u}}\|_{H^1(D_{\mathrm{ref}})} \leq \frac{C_1}{4}|\boldsymbol{\alpha}|!\boldsymbol{\mu}^{\boldsymbol{\alpha}} + \frac{C_1}{4}\sum_{\boldsymbol{\alpha}' < \boldsymbol{\alpha}} \binom{\boldsymbol{\alpha}}{\boldsymbol{\alpha}'} |\boldsymbol{\alpha} - \boldsymbol{\alpha}'|! \boldsymbol{\mu}^{\boldsymbol{\alpha}-\boldsymbol{\alpha}'} \|\partial_{\boldsymbol{y}}^{\boldsymbol{\alpha}'} \hat{\boldsymbol{u}}\|_{H^1(D_{\mathrm{ref}})}, \tag{3.6}$$

where

$$C_1 = 8\frac{\overline{\lambda}^2}{\underline{\lambda}^d} C' C_{\mathbb{C}} \max\{C_D + C_\Gamma, C_{\mathbb{C}}\}.$$

The proof is now by induction on $|\boldsymbol{\alpha}|$. The induction hypothesis is given by

$$\|\partial_{\boldsymbol{y}}^{\boldsymbol{\alpha}} \hat{\boldsymbol{u}}\|_{H^1(D_{\mathrm{ref}})} \leq C_1^{|\boldsymbol{\alpha}|+1}|\boldsymbol{\alpha}|!\boldsymbol{\mu}^{\boldsymbol{\alpha}}. \tag{3.7}$$

Base case. Let us consider $\boldsymbol{\alpha} = \mathbf{0}$. Then, by using (3.4), Lemmata A.2 and A.3, we derive from Corollary 2.8 the result

$$\|\hat{\boldsymbol{u}}\|_{H^1(D_{\mathrm{ref}})} \leq 2C_{\mathbb{C}}\frac{\overline{\lambda}^2}{\underline{\lambda}^d} C_{\mathrm{det}}\left(C_D C_f + C_\Gamma \frac{C_g}{\underline{\lambda}}\right) \leq C_1,$$

which proves the base case.

Induction step. Now, for some $n \geq 1$, let the induction hypothesis (3.7) hold for all $|\boldsymbol{\alpha}'| \leq n-1$. Then, in view of (3.6), we have for $|\boldsymbol{\alpha}| = n$ that

$$
\begin{aligned}
\|\partial_{\boldsymbol{y}}^{\boldsymbol{\alpha}} \hat{\boldsymbol{u}}\|_{H^1(D_{\mathrm{ref}})} &\leq \frac{C_1}{4}|\boldsymbol{\alpha}|!\boldsymbol{\mu}^{\boldsymbol{\alpha}} + \frac{C_1}{4}\sum_{\boldsymbol{\alpha}'<\boldsymbol{\alpha}} \binom{\boldsymbol{\alpha}}{\boldsymbol{\alpha}'}|\boldsymbol{\alpha}-\boldsymbol{\alpha}'|!\boldsymbol{\mu}^{\boldsymbol{\alpha}-\boldsymbol{\alpha}'}|\boldsymbol{\alpha}'|!\boldsymbol{\mu}^{\boldsymbol{\alpha}'}C_1^{|\boldsymbol{\alpha}'|+1} \\
&\leq \frac{C_1}{4}|\boldsymbol{\alpha}|!\boldsymbol{\mu}^{\boldsymbol{\alpha}} + \frac{C_1}{4}\boldsymbol{\mu}^{\boldsymbol{\alpha}}\sum_{\boldsymbol{\alpha}'<\boldsymbol{\alpha}} \binom{\boldsymbol{\alpha}}{\boldsymbol{\alpha}'}|\boldsymbol{\alpha}-\boldsymbol{\alpha}'|!|\boldsymbol{\alpha}'|!C_1^{|\boldsymbol{\alpha}'|+1} \\
&= \frac{C_1}{4}|\boldsymbol{\alpha}|!\boldsymbol{\mu}^{\boldsymbol{\alpha}} + \frac{C_1}{4}\boldsymbol{\mu}^{\boldsymbol{\alpha}}\sum_{j=0}^{|\boldsymbol{\alpha}|-1}\sum_{\substack{\boldsymbol{\alpha}'<\boldsymbol{\alpha}\\|\boldsymbol{\alpha}'|=j}} \binom{\boldsymbol{\alpha}}{\boldsymbol{\alpha}'}|\boldsymbol{\alpha}-\boldsymbol{\alpha}'|!|\boldsymbol{\alpha}'|!C_1^{|\boldsymbol{\alpha}'|+1}.
\end{aligned}
$$

Using the combinatorial identity

$$
\sum_{\substack{\boldsymbol{\alpha}'\leq\boldsymbol{\alpha}\\|\boldsymbol{\alpha}'|=j}} \binom{\boldsymbol{\alpha}}{\boldsymbol{\alpha}'} = \binom{|\boldsymbol{\alpha}|}{j}
$$

and the inequality (see [15, Lemma 9])

$$
\frac{C_1}{2}\frac{C_1^{|\boldsymbol{\alpha}|}}{C_1-1} \leq C_1^{|\boldsymbol{\alpha}|},
$$

we obtain estimate

$$
\begin{aligned}
\|\partial_{\boldsymbol{y}}^{\boldsymbol{\alpha}} \hat{\boldsymbol{u}}\|_{H^1(D_{\mathrm{ref}})} &\leq \frac{C_1}{4}|\boldsymbol{\alpha}|!\boldsymbol{\mu}^{\boldsymbol{\alpha}} + \frac{C_1}{4}\boldsymbol{\mu}^{\boldsymbol{\alpha}}\sum_{j=0}^{|\boldsymbol{\alpha}|-1}\binom{|\boldsymbol{\alpha}|}{j}(|\boldsymbol{\alpha}|-j)!|j!C_1^{j+1} \\
&= \frac{C_1}{4}|\boldsymbol{\alpha}|!\boldsymbol{\mu}^{\boldsymbol{\alpha}} + \frac{C_1}{4}\boldsymbol{\mu}^{\boldsymbol{\alpha}}|\boldsymbol{\alpha}|!C_1\sum_{j=0}^{|\boldsymbol{\alpha}|-1}C_1^j \\
&\leq \frac{C_1}{4}|\boldsymbol{\alpha}|!\boldsymbol{\mu}^{\boldsymbol{\alpha}} + \frac{1}{4}|\boldsymbol{\alpha}|!\boldsymbol{\mu}^{\boldsymbol{\alpha}}C_1\frac{C_1^{|\boldsymbol{\alpha}|}}{C_1-1} \leq \frac{C_1}{4}|\boldsymbol{\alpha}|!\boldsymbol{\mu}^{\boldsymbol{\alpha}} + \frac{C_1^{|\boldsymbol{\alpha}|}}{2}|\boldsymbol{\alpha}|!\boldsymbol{\mu}^{\boldsymbol{\alpha}}.
\end{aligned}
$$

Since $C_1 > 1$, we conclude

$$
\|\partial_{\boldsymbol{y}}^{\boldsymbol{\alpha}} \hat{\boldsymbol{u}}\|_{H^1(D_{\mathrm{ref}})} \leq \frac{C_1^{|\boldsymbol{\alpha}|+1}}{4}|\boldsymbol{\alpha}|!\boldsymbol{\mu}^{\boldsymbol{\alpha}} + \frac{C_1^{|\boldsymbol{\alpha}|+1}}{2}|\boldsymbol{\alpha}|!\boldsymbol{\mu}^{\boldsymbol{\alpha}} \leq C_1^{|\boldsymbol{\alpha}|+1}|\boldsymbol{\alpha}|!\boldsymbol{\mu}^{\boldsymbol{\alpha}}.
$$

This completes the proof with $C_2 := C''$. ■

4. Numerical experiments. In this part, we present numerical results illustrating and validating our findings. First, we choose some reference domain and covariance kernel. Then, we compute the truncated Karhunen-Loève expansion $\boldsymbol{V}$ in order to define the random domain $\boldsymbol{V}(D_{\mathrm{ref}})$. Finally, we consider the linear elasticity problem on the random domain.

Then, we use both, sparse grid quadrature [3, 24] and quasi-Monte Carlo quadrature [23] for numerical quadrature in the high-dimensional unit cube associated with the random parameters. Particularly, we apply the anisotropic sparse grid quadrature based on Gauss-Legendre points proposed in [12]. Moreover, we apply the quasi-Monte Carlo quadrature with interlaced Sobol points and Halton points mapped onto the hypercube $[-1/2, 1/2]^M$, compare [21, 22, 25]. All these quadrature methods have in common that they converge dimension independent provided that the weights $\{\gamma_k\}$ of the solution's derivatives, which are inhereted from the Karhunen-Loève expansion, decay sufficiently fast algebraically.

4.1. Physical model. We consider a body with an interior random interface. The reference domain is chosen as the square

$$D_{\text{ref}} = [-1, 1] \times [-1, 1].$$

The bottom boundary of this reference domain is fixed, i.e. we have the Dirichlet boundary condition $\boldsymbol{u} = 0$ there. On the top boundary of D_{ref}, we apply the surface force $\boldsymbol{g} = (0, -1)$. The right and left boundary of D_{ref} is free, which means that we have there the homogeneous Neumann boundary condition $\partial\boldsymbol{u}/\partial\boldsymbol{n} = 0$. The body force is taken as $\boldsymbol{f} = (0, 0)$. We refer to the left-hand side of Figure 1 for an illustration of this setup.

We further consider an inclusion $S_{\text{ref}} \subset D_{\text{ref}}$ given by

$$S_{\text{ref}} = \{\boldsymbol{x} \in D_{\text{ref}} : \|\boldsymbol{x}\| \leq 0.5\}.$$

The material of the body in $D_{\text{ref}} \setminus \overline{S_{\text{ref}}}$ is considered to be steel with Young modulus and Poisson ratio of

$$E_0 = 20, \quad \nu_0 = 0.28$$

and the material of the body inside the inclusion S_{ref} is considered to be an aluminium alloy with

$$E_1 = 6.9, \quad \nu_1 = 0.33.$$

Therefore, the general material coefficients are

$$E = E_0 \mathbb{1}_{D_{\text{ref}}\setminus\overline{S_{\text{ref}}}} + \mathbb{E}_1 \mathbb{1}_{S_{\text{ref}}} \quad \text{and} \quad \nu = \nu_0 \mathbb{1}_{D_{\text{ref}}\setminus\overline{S_{\text{ref}}}} + \nu_1 \mathbb{1}_{S_{\text{ref}}}.$$

The isotropic linear elasticity model can be described by the following nonhomogeneous stress tensor

$$\begin{aligned}
\sigma_{11}(\boldsymbol{u}) &= (2\mu + \lambda)\varepsilon_{11}(\boldsymbol{u}) + \lambda\varepsilon_{22}(\boldsymbol{u}), \\
\sigma_{12}(\boldsymbol{u}) &= \sigma_{21}(\boldsymbol{u}) = 2\mu\varepsilon_{12}(\boldsymbol{u}), \\
\sigma_{22}(\boldsymbol{u}) &= \lambda\varepsilon_{11}(\boldsymbol{u}) + (2\mu + \lambda)\varepsilon_{22}(\boldsymbol{u})
\end{aligned}$$

with the Lamé constants

$$\mu = \frac{E}{2(1+\nu)}, \quad \lambda = \frac{E\nu}{(1+\nu)(1-2\nu)}.$$

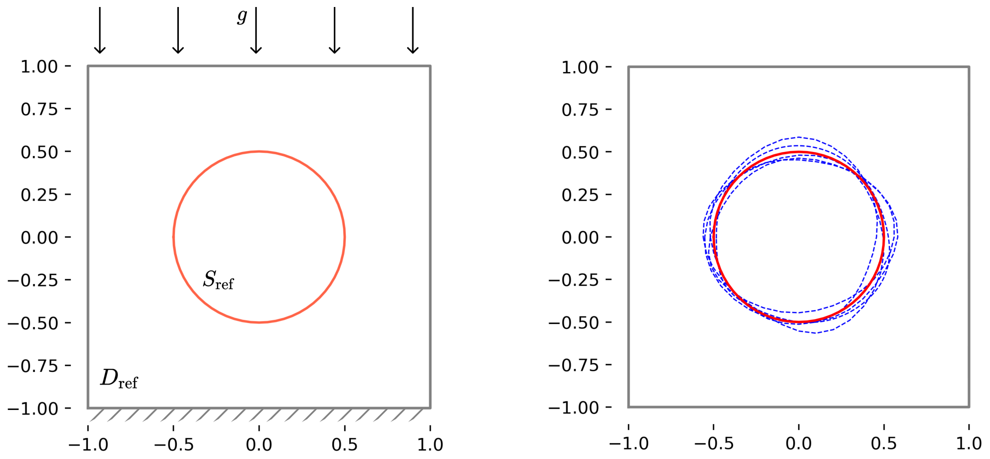

Figure 1. *Reference domain and five samples of pseudo-random domains with Halton points.*

4.2. Stochastic model. We consider a random field $\boldsymbol{V}(\boldsymbol{x},\omega)$ which is described by the mean $\mathbb{E}[\boldsymbol{V}](\boldsymbol{x}) = \boldsymbol{x}$ and the covariance function

$$\operatorname{Cov}[\boldsymbol{V}](\boldsymbol{x},\boldsymbol{x}') = \frac{1}{100} B(\boldsymbol{x})B(\boldsymbol{x}') \begin{bmatrix} g_{11}(\boldsymbol{x},\boldsymbol{x}')n_{11}(\boldsymbol{x},\boldsymbol{x}') & g_{12}(\boldsymbol{x},\boldsymbol{x}')n_{12}(\boldsymbol{x},\boldsymbol{x}') \\ g_{21}(\boldsymbol{x},\boldsymbol{x}')n_{21}(\boldsymbol{x},\boldsymbol{x}') & g_{22}(\boldsymbol{x},\boldsymbol{x}')n_{22}(\boldsymbol{x},\boldsymbol{x}') \end{bmatrix},$$

where

$$\begin{aligned} g_{11}\boldsymbol{x},\boldsymbol{x}') &= 5\exp(-4|\boldsymbol{x}-\boldsymbol{x}'|^2), \quad & g_{12}(\boldsymbol{x},\boldsymbol{x}') &= \exp(-0.1|2\boldsymbol{x}-\boldsymbol{x}'|^2), \\ g_{21}(\boldsymbol{x},\boldsymbol{x}') &= \exp(-0.1|\boldsymbol{x}-2\boldsymbol{x}'|^2), \quad & g_{22}(\boldsymbol{x},\boldsymbol{x}') &= 5\exp(-|\boldsymbol{x}-\boldsymbol{x}'|^2), \end{aligned}$$

and

$$\begin{aligned} n_{11}(\boldsymbol{x},\boldsymbol{x}') &= \cos(\theta_{\boldsymbol{x}})\cos(\theta_{\boldsymbol{x}'}), \quad & n_{12}(\boldsymbol{x},\boldsymbol{x}') &= \cos(\theta_{\boldsymbol{x}})\sin(\theta_{\boldsymbol{x}'}), \\ n_{21}(\boldsymbol{x},\boldsymbol{x}') &= \sin(\theta_{\boldsymbol{x}})\cos(\theta_{\boldsymbol{x}'}), \quad & n_{22}(\boldsymbol{x},\boldsymbol{x}') &= \sin(\theta_{\boldsymbol{x}})\sin(\theta_{\boldsymbol{x}'}). \end{aligned}$$

As we want to consider shape uncertainties only in the interior of the reference domain, we use the blending function $B(\boldsymbol{x})$, such that $B(\boldsymbol{x})|_{\Gamma_{\text{ref}}} = 0$ and $B(\boldsymbol{x})|_{\partial S_{\text{ref}}} = 1$. In our implementation, we choose $B(\boldsymbol{x}) = \frac{4}{3}B_2(5|\boldsymbol{x} - P\boldsymbol{x}|)$, where B_2 is the cardinal quadratic B-spline on the partition of step size 1, centered in 0, and $P\boldsymbol{x}$ denotes the orthogonal projection of $\boldsymbol{x}$ onto the circular interface S_{ref}. In order to illustrate the difference between the random interfaces and the reference interface that this setup for the random domain mapping then yields, we display five exemplary samples of pseudo-random interfaces using Halton points on the right-hand side of Figure 1.

4.3. Discretization. We consider a standard finite element discretisation of the physical model with a triangulation of the reference domain D_{ref} that resolves the reference interface and utilises continuous element-wise linear finite elements. For the implementation, we use FreeFEM with 46 078 finite elements, see [18].

To compute the Karhunen-Loève expansion, we discretize the restriction of the covariance operator $\mathcal{C}_{\boldsymbol{V}}$ from (2.7) by using the matrix function $\operatorname{Cov}[\boldsymbol{V}](\boldsymbol{x},\boldsymbol{x}')$ taken in the mesh vertices $\{\boldsymbol{x}_i\}_{i=1}^N$ and the finite element mass matrix $\boldsymbol{G}$. This amounts to the solution of the generalized eigenvalue problem

$$\boldsymbol{GCG\phi} = \lambda \boldsymbol{G\phi}, \quad \text{where } \boldsymbol{C} = \big[\operatorname{Cov}(\boldsymbol{x}_i,\boldsymbol{x}_j)\big]_{i,j=1}^N \text{ and } \boldsymbol{G} = \big[(\varphi_i,\varphi_j)_{L^2(D_{\mathrm{ref}})}\big]_{i,j=1}^N,$$

and finally leads to the discrete Karhunen-Loève expansion

$$\boldsymbol{V}(\boldsymbol{x},\boldsymbol{y}) = \boldsymbol{x} + 2\sum_{k=1}^{M}\sqrt{3\lambda_k}\boldsymbol{\phi}_k(\boldsymbol{x})y_k.$$

To solve the generalized eigenvalue problem efficiently, we do not compute $\boldsymbol{C}$ but directly compute its truncated pivoted Cholesky decomposition, which yields a low-rank approximation of $\boldsymbol{C}$ and hence enables a fast eigenpair computation, see [14] for the details. Since the eigenvalues are exponentially decreasing with the rate $\gamma_k \approx \exp(-0.1k)$, compare Figure 2, it was enough for us to truncate the pivoted Cholesky decomposition with $M = 100$, which results in a relative error of the trace norm of the order 10^{-6}.

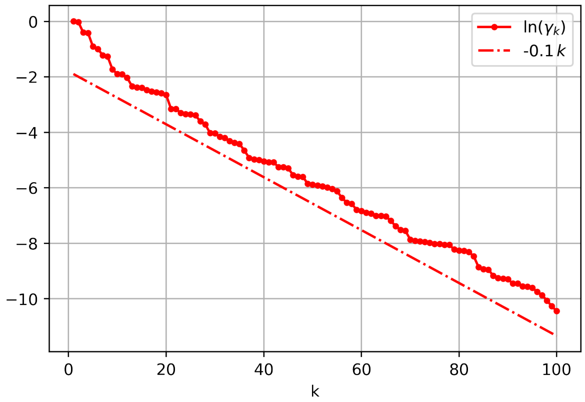

Figure 2. *The dimension weights $\{\gamma_k\}$ with respect to a logarithmic scale. The weights decay exponentially.*

We focus on the displacement field $\boldsymbol{u}$ and the von Mises stress $\sigma^*(\boldsymbol{u})$ in accordance with

$$\sigma^* = \sqrt{\sigma_{11}^2 - \sigma_{11}\sigma_{22} + \sigma_{22}^2 + 3\sigma_{12}^2}$$

as the quantities of interest (QoI). The approximation of the expectation and variance of the displacement field using a quadrature rule is then given by

$$\begin{aligned}\mathbb{E}[\hat{\boldsymbol{u}}](\boldsymbol{x}) &\approx Q_l[\hat{\boldsymbol{u}}](\boldsymbol{x}) := \sum_{i=1}^{N_l} w_i \hat{\boldsymbol{u}}(\boldsymbol{x},\boldsymbol{y}^i),\\ \mathbb{V}[\hat{\boldsymbol{u}}](\boldsymbol{x}) &\approx V_l[\hat{\boldsymbol{u}}](\boldsymbol{x}) := Q_l[\hat{\boldsymbol{u}}(\boldsymbol{x})\otimes\hat{\boldsymbol{u}}(\boldsymbol{x})] - Q_l[\hat{\boldsymbol{u}}(\boldsymbol{x})]\otimes Q_l[\hat{\boldsymbol{u}}(\boldsymbol{x})],\end{aligned}$$

while for the von Mises stress we have

$$\mathbb{E}[\sigma^*(\hat{\boldsymbol{u}})](\boldsymbol{x}) \approx Q_l[\sigma^*(\hat{\boldsymbol{u}})](\boldsymbol{x}) := \sum_{i=1}^{N_l} w_i \sigma^*\big(\hat{\boldsymbol{u}}(\boldsymbol{x}, \boldsymbol{y}^i)\big),$$
$$\mathbb{V}[\sigma^*(\hat{\boldsymbol{u}})](\boldsymbol{x}) \approx V_l[\sigma^*(\hat{\boldsymbol{u}})](\boldsymbol{x}) := Q_l[\sigma^*(\hat{\boldsymbol{u}})^2](\boldsymbol{x}) - \big(Q_l[\sigma^*(\hat{\boldsymbol{u}})](\boldsymbol{x})\big)^2.$$

Here, $w_i \in \mathbb{R}$, $i = 1, \ldots, N_l$, are the quadrature weights and $\boldsymbol{y}^i \in \square$ the quadrature points.

We choose the quadrature points $\boldsymbol{y}^i = (\boldsymbol{\xi}^i - 1/2)$, $i = 1, \ldots, M$, as a mapped sequence of the anisotropic sparse grid quadrature over $[0, 1]$, see [12][1], interlaced Sobol points with interlacing factor $\alpha = 2$, compare [22][2], and Halton points, which amounts to a series of domains $D(\boldsymbol{y}^i) = \boldsymbol{V}(D_{\text{ref}}, \boldsymbol{y}^i)$. In the case of interlaced Sobol points and Halton points, the weights are simply given by $w_i = 1/N_l$ for all $i = 1, \ldots, N_l$. In the case of the anisotropic sparse grid quadrature, the weights are computed for each corresponding sequence of y_i.

4.4. Numerical results. We first solve the problem on the reference domain D_{ref} without any uncertainties, i.e. using the expected domain mapping. For the visualization, we present the distribution of the von Mises stress and the pointwise ℓ^2-norm of the displacement field $\boldsymbol{u}$ inside the body, i.e,

$$\|\boldsymbol{u}(\boldsymbol{x})\| = \sqrt{u_1^2(\boldsymbol{x}) + u_2^2(\boldsymbol{x})}, \quad \boldsymbol{x} \in D_{\text{ref}}.$$

The results are found in Figure 3 in the left column. Whereas, in the right column, one can find the related quantities $\widehat{\boldsymbol{u}}$ and $\sigma^*(\widehat{\boldsymbol{u}})$ for one Halton sample of the random domain mapping. By comparing these, one can get an impression of the effect of the randomness in the domain.

For our numerical experiments, the anisotropic sparse grid quadrature on level $l_{SG} = 7$, which yields a quadrature rule with $N_l = 17\,931$ points, serves as the reference solution in order to examine the convergence behaviour of the different quadrature methods. It should be noted that variance of the displacement field is a matrix of size 2×2, so for a visualization and also for measuring the convergence rates, we use the Frobenius norm. The respective approximate expectations and variances of the von Mises stress and the displacement field are found in Figure 4.

[1] We use the implementation of anisotropic sparse grid quadrature available from https://github.com/muchip/SPQR.

[2] We use the implementation of lattice rules for quasi-Monte Carlo quadrature available from https://people.cs.kuleuven.be/~dirk.nuyens/qmc4pde.

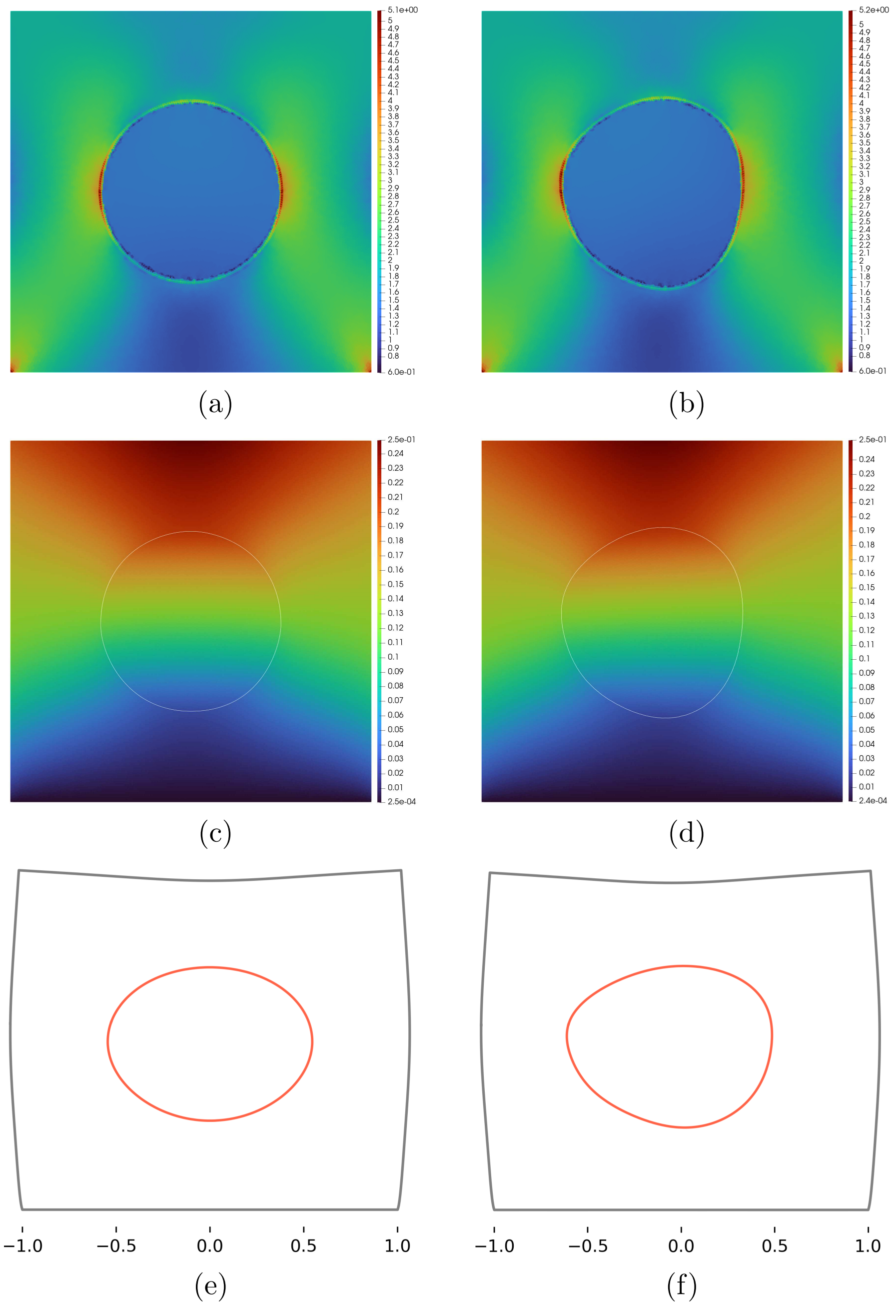

Figure 3. *The solution on the reference domain without uncertainties (left column) and for a specific Halton sample (right column): (a)&(b) von Mises stress* $\sigma^*(\boldsymbol{u}(\boldsymbol{x}))$*; (c)&(d) pointwise norm* $\|\boldsymbol{u}(\boldsymbol{x})\|$ *of the displacement; (e)&(f) domain deformed by the displacement field* $\boldsymbol{u}(\boldsymbol{x})$*.*

In our convergence studies, we apply $N_l = 4 \cdot 2^{l_{QMC}}$ interlaced Sobol points and Halton points, respectively, on the level $l_{QMC} = 1, \ldots, 10$ and 6 levels of sparse grid quadrature points, which means $N_l = 5, 21, 121, 447, 1649, 5561$ points. Figure 5 (a) and (c) depict respectively the error in the L^2-norm of the expected displacement field and the expected von Misses

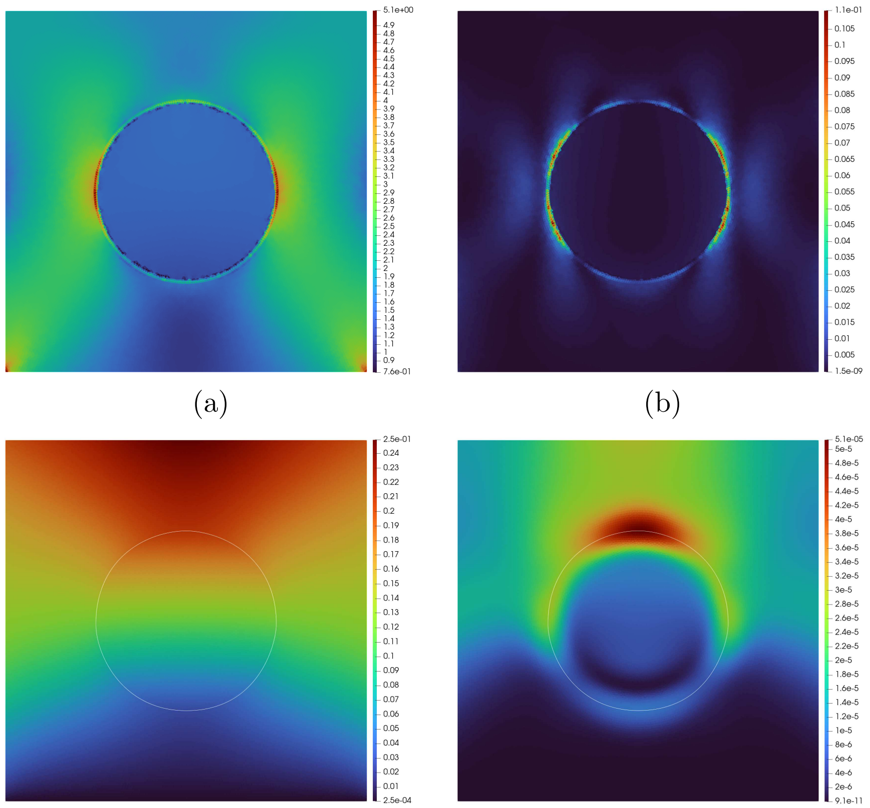

(a) (b) (c) (d)

Figure 4. *Approximate expectations and variances for $l_{SG} = 7$ of the von Mises stress and the displacement field on the reference domain: (a) expectation $Q_{l_{SG}}[\sigma^*(\hat{\boldsymbol{u}})](\boldsymbol{x})$ of the von Mises stress; (b) variance $V_{l_{SG}}[\sigma^*(\hat{\boldsymbol{u}})](\boldsymbol{x})$ of the von Mises stress; (c) pointwise norm of the expected displacement, $\|Q_{l_{SG}}[\hat{\mathbf{u}}](\boldsymbol{x})\|$; (d) pointwise norm of the variance of the displacement, $\|V_{l_{SG}}[\hat{\mathbf{u}}](\boldsymbol{x})\|_F$.*

stress versus the related cost, which is given by the number N_l of samples. As can be figured out from Figure 5 (c), the convergence rate for the mean of the displacement field is $N_l^{-0.84}$ for the Halton points and $N_l^{-1.19}$ for the interlaced Sobol points. For the anisotropic sparse grid quadrature, we observe nearly the same rate: $N_l^{-1.23}$. Basically the same rates are also observed for the mean of the von Mises stress, compare Figure 5 (a). In addition, in Figure 5 (b) and (d), there are also the errors and the related convergence rates presented for the variance of the QoI's measured in the L^1-norm. Also these convergence rates basically agree with the convergence rates observed for the respective means.

5. Conclusion. The presented analysis was concerned with the regularity of the solution to the equations of linear elasticity in the presence of domain uncertainties. The random domain under consideration was modelled by means of the Karhunen-Loève expansion of the random domain mapping defined on a fixed, nominal domain. We have proven analytic dependency of the random solution on the random input parameters. Especially, we have established decay estimates for the solution's derivatives with respect to the dimension of the random

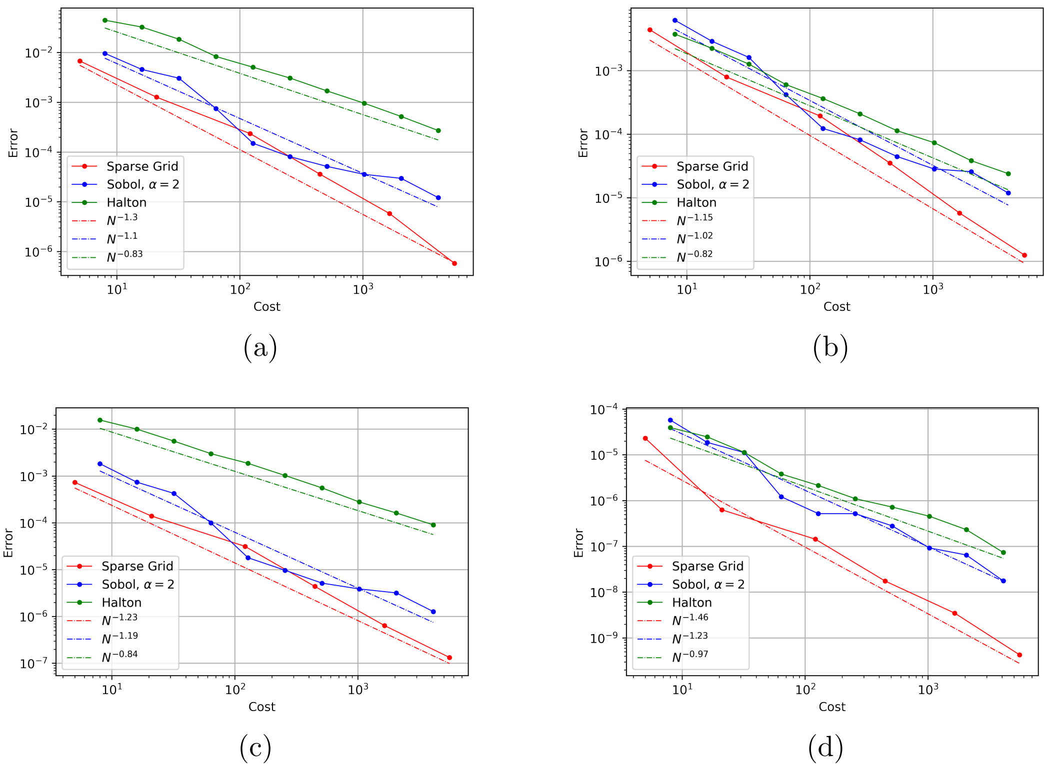

Figure 5. *The convergence rate and errors: (a) $Q_l[\sigma^*(\hat{\boldsymbol{u}})](\boldsymbol{x})$ measured in $L^2(D_{\text{ref}})$; (b) $V_l[\sigma^*(\hat{\boldsymbol{u}})](\boldsymbol{x})$ measured in $L^1(D_{\text{ref}})$. (c) $Q_l[\hat{\boldsymbol{u}}](\boldsymbol{x})$ measured in $L^2(D_{\text{ref}})$; (d) $V_l[\hat{\boldsymbol{u}}](\boldsymbol{x})$ measured in $L^1(D_{\text{ref}})$.*

inputs which enable dimension robust quadrature methods for the random parameters. Our theoretical findings were validated by numerical experiments.

Acknowledgments. The authors are pleased to thank Christoph Schwab (ETH Zurich) for the stimulating discussion and helpful remarks which helped to realize the present results.

Appendix. The appendix is devoted to three lemmata required in the proof of the main result concerning the random solution's regularity. The first lemma is dedicated to the derivatives estimate of matrix

$$A(\boldsymbol{x},\boldsymbol{y}) = \det \boldsymbol{J}(\boldsymbol{x},\boldsymbol{y})\big(\boldsymbol{J}^\top(\boldsymbol{x},\boldsymbol{y})\boldsymbol{J}(\boldsymbol{x},\boldsymbol{y})\big)^{-1}.$$

Lemma A.1 (see [15, Theorem 3]). *Let $\boldsymbol{V}$ be given as in (2.8). Then, the derivatives of A satisfy*

$$\big|\big|\big|\partial_{\boldsymbol{y}}^{\boldsymbol{\alpha}} A\big|\big|\big|_\infty \leq (|\boldsymbol{\alpha}|+1)!\frac{C_{\text{det}}}{\underline{\lambda}^2}\left(\frac{2(1+C_{\boldsymbol{\gamma}})}{\underline{\lambda}^2\log 2}\right)^{|\boldsymbol{\alpha}|}\boldsymbol{\gamma}^{\boldsymbol{\alpha}}, \tag{A.1}$$

where

$$C_{\text{det}} = 2(1+\overline{\lambda})^d, \quad C_{\boldsymbol{\gamma}} = \sum_{k=1}^M \gamma_k,$$

and the norm $|||\cdot|||_\infty$ *is defined in* (3.1).

The next lemma presents a regularity result for the volume force

$$\widetilde{f}(\boldsymbol{x},\boldsymbol{y}) = \det \boldsymbol{J}(\boldsymbol{x},\omega)\hat{\boldsymbol{f}}(\boldsymbol{x},\omega).$$

Lemma A.2 (see [15, Theorem 4]). *Let* $\hat{\boldsymbol{f}} \in C^\infty(\mathcal{D})$ *be analytic, i.e.*

$$\|\partial_{\boldsymbol{x}}^{\boldsymbol{\alpha}}\hat{\boldsymbol{f}}\|_{L^\infty(\mathcal{D};\mathbb{R}^d)} \le |\boldsymbol{\alpha}|!\rho_f^{-|\boldsymbol{\alpha}|}C_f$$

for all $\boldsymbol{\alpha} \in \mathbb{N}_0 \times \mathbb{N}_0$ *and some* $\rho_f \in (0,1]$*. Then, the derivatives of* $\widetilde{f}(\boldsymbol{x},\boldsymbol{y})$ *satisfy*

$$\|\partial_{\boldsymbol{y}}^{\boldsymbol{\alpha}}\widetilde{\boldsymbol{f}}\|_{L^\infty(\square;L^\infty(D_{\mathrm{ref}}))} \le (|\boldsymbol{\alpha}|+1)!C_f C_{\det}\left(\frac{d}{\rho_f \log 2}\right)^{|\boldsymbol{\alpha}|}\boldsymbol{\gamma}^{\boldsymbol{\alpha}}. \tag{A.2}$$

Finally, we need also an estimate for derivatives of mapped surface force

$$\widetilde{g}(\boldsymbol{x},\boldsymbol{y}) = \left\|\boldsymbol{J}^{-\top}(\boldsymbol{x},\omega)\boldsymbol{n}_{\mathrm{ref}}(x)\right\| \det \boldsymbol{J}(\boldsymbol{x},\omega)\hat{\boldsymbol{g}}(\boldsymbol{x},\omega).$$

Lemma A.3. *Let* $\hat{\boldsymbol{g}} \in C^\infty(\mathcal{G}^N)$ *be analytic, i.e.*

$$\|\partial_{\boldsymbol{x}}^{\boldsymbol{\alpha}}\hat{\boldsymbol{g}}\|_{L^\infty(\mathcal{G}^N;\mathbb{R}^d)} \le |\boldsymbol{\alpha}|!\rho_g^{-|\boldsymbol{\alpha}|}C_g$$

for all $\boldsymbol{\alpha} \in \mathbb{N}_0 \times \mathbb{N}_0$ *and some* $\rho_g \in (0,1]$*. Then, the derivatives of* $\widetilde{\boldsymbol{g}}(\boldsymbol{x},\boldsymbol{y})$ *satisfy the estimate*

$$\|\partial_{\boldsymbol{y}}^{\boldsymbol{\alpha}}\widetilde{\boldsymbol{g}}\|_{L^\infty(\square;L^\infty(\Gamma_{\mathrm{ref}}^N))} \le (|\boldsymbol{\alpha}|+2)!\frac{C_g C_{\det}}{2\underline{\lambda}}\left(\frac{d}{\underline{\lambda}\rho_g(\log 2)^2}\right)^{|\boldsymbol{\alpha}|}\boldsymbol{\gamma}^{\boldsymbol{\alpha}}. \tag{A.3}$$

Proof. The proof of this lemma technically repeats the proof of the previous two lemmata, compare [15]. ∎

REFERENCES

[1] Hans Wilhelm Alt. *Linear Functional Analysis. An Application-Oriented Introduction.* Springer, Berlin-Heidelberg, 2016.

[2] Dietrich Braess. *Finite Elements. Theory, Fast Solvers, and Applications in Solid Mechanics.* Cambridge University Press, Cambridge, second edition, 2001.

[3] Hans-Joachim Bungartz and Michael Griebel. Sparse grids. *Acta Numerica*, 13:147–269, 2004.

[4] Julio E. Castrillón-Candás, Fabio Nobile, and Raul F. Tempone. Analytic regularity and collocation approximation for elliptic PDEs with random domain deformations. *Computers and Mathematics with Applications*, 71(6):1173–1197, 2016.

[5] Philippe G. Ciarlet. *Mathematical Elasticity. Volume I: Three-Dimensional Elasticity*, volume 20 of *Studies in Mathematics and its Applications.* North Holland, Amsterdam, 1988.

[6] Albert Cohen, Christoph Schwab, and Jakob Zech. Shape holomorphy of the stationary Navier-Stokes equations. *SIAM Journal on Mathematical Analysis*, 50(2):1720–1752, 2018.

[7] Marc Dambrine, Isabelle Greff, Helmut Harbrecht, and Benedicte Puig. Numerical solution of the Poisson equation with a thin layer of random thickness. *SIAM Journl on Numerical Analysis*, 54(2):921–941, 2016.

[8] Jürgen Dölz, Helmut Harbrecht, Carlos Jerez-Hanckes, and Michael D. Multerer. Isogeometric multilevel quadrature for forward and inverse random acoustic scattering. *Computer Methods in Applied Mechanics and Engineering*, 388:114242, 2022.

[9] Robert N. Gantner and Michael Peters. Higher order quasi-Monte Carlo for Bayesian shape inversion. *SIAM/ASA Journal on Uncertainty Quantification*, 6(2):707–736, 2018.

[10] Michael Griebel and Helmut Harbrecht. Approximation of bi-variate functions. Singular value decomposition versus sparse grids. *IMA Journal of Numerical Analysis*, 34(1):28–54, 2014.

[11] Michael Griebel and Helmut Harbrecht. Singular value decomposition versus sparse grids. refined complexity estimates. *IMA Journal of Numerical Analysis*, 39(4):1652–1671, 2019.

[12] Abdul-Lateef Haji-Ali, Helmut Harbrecht, Michael D. Peters, and Markus Siebenmorgen. Novel results for the anisotropic sparse grid quadrature. *Journal of Complexity*, 47:62–85, 2018.

[13] Helmut Harbrecht and Michael Peters. The second order perturbation approach for PDEs on random domains. *Applied Numerical Mathematics*, 125:159–171, 2018.

[14] Helmut Harbrecht, Michael Peters, and Markus Siebenmorgen. Efficient approximation of random fields for numerical applications. *Numerical Linear Algebra with Applications*, 22(4):596–617, 2015.

[15] Helmut Harbrecht, Michael Peters, and Markus Siebenmorgen. Analysis of the domain mapping method for elliptic diffusion problems on random domains. *Numerische Mathematik*, 134(4):823–856, 2016.

[16] Helmut Harbrecht and Marc Schmidlin. Multilevel quadrature for elliptic problems on random domains by the coupling of FEM and BEM. *Stochastics and Partial Differential Equations: Analysis and Computations*, 10:1619–1650, 2022.

[17] Helmut Harbrecht, Reinhold Schneider, and Christoph Schwab. Sparse second moment analysis for elliptic problems in stochastic domains. *Numerische Mathematik*, 109(3):385–414, 2008.

[18] Frederic Hecht. New development in freefem++. *Journal of Numerical Mathematics*, 20(3-4):251–265, 2012.

[19] Ralf Hiptmair, Laura Scarabosio, Claudia Schillings, and Christoph Schwab. Large deformation shape uncertainty quantification in acoustic scattering. *Advances in Computational Mathematics*, 44(5):1475–1518, 2018.

[20] Carlos Jerez-Hanckes, Christoph Schwab, and Jakob Zech. Electromagnetic wave scattering by random surfaces: Shape holomorphy. *Mathematical Models and Methods in Applied Sciences*, 27(12):2229–2259, 2017.

[21] Stephen Joe and Frances Y. Kuo. Constructing Sobol' sequences with better two-dimensional projections. *SIAM Journal on Scientific Compututing*, 30:2635–2654, 2008.

[22] Frances Y. Kuo and Dirk Nuyens. Application of quasi-Monte Carlo methods to elliptic PDEs with random diffusion coefficients: a survey of analysis and implementation. *Foundations of Computational Mathematics*, 16:1631–1696, 2016.

[23] Harald Niederreiter. *Random Number Generation And Quasi-Monte Carlo Methods*. Society for Industrial and Applied Mathematics, Philadelphia, 1992.

[24] Sergei A. Smolyak. Quadrature and interpolation formulas for tensor products of certain classes of functions. *Soviet Mathematics*, 4:240–243, 1963. Translation of Doklady Akademii Nauk SSSR.

[25] Xiaoqun Wang. A constructive approach to strong tractability using quasi-Monte Carlo algorithms. *Journal of Complexity*, 18:683–701, 2002.

[26] Dongbin Xiu and Daniel M. Tartakovsky. Numerical methods for differential equations in random domains. *SIAM Journal on Scientific Computing*, 28(3):1167–1185, 2006.